JOURNAL OF SOLID STATE CHEMISTRY 54, 389–399 (1984)

# Stabilization of Unusual Electronic Configurations of Transition Elements in Elongated Six-Coordinated Oxygen Sites of a $K_2NiF_4$ Structure*

GÉRARD DEMAZEAU, BERNARD BUFFAT, MICHEL POUCHARD, AND PAUL HAGENMULLER

*Laboratoire de Chimie du Solide du CNRS, 351, cours de la Libération, 33405 Talence Cedex, France*

Received December 30, 1983

The $A'_xA_{2-x}Li_{0.5}M_{0.5}O_4$ matrix deriving from the $K_2NiF_4$ structure has an elongated $MO_6$ octahedron; it has been used to stabilize anisotropic electronic configurations such as high-spin $Fe^{4+}$, low-spin $Co^{4+}$, medium-spin $Co^{3+}$, low-spin $Ni^{3+}$, or low-spin $Cu^{3+}$. The choice of ions to be stabilized was based on a simple model for predicting the electronic configuration of a $d^n$ ion in a tetragonally distorted octahedral environment. 

## Introduction

Recently we have proposed a simple model for predicting the electronic configuration of a $d^n$ ion in a tetragonally distorted octahedral environment (*1*). This model is based on the Tanabe–Sugano diagrams, which give the relative energy vs $Dq/B$ of the different spectroscopic terms corresponding to an electronic population $d^n$ in an $O_h$ symmetry. In the case of lower symmetry, e.g., $D_{4h}$, a derived diagram giving the stability domains of the different electronic configurations can be drawn. It is based on the criteria: (a) the energy of the different terms varies linearly with $Dq$ (i.e., mixing of the different terms is neglected); (b) the crystal field parameter $Dq$ is directly proportional to $(d_{c-a})^{-5}$, $d_{c-a}$ being the cation–anion distance; (c) the average value of $d_{c-a}$, e.g., $\overline{d}_{c-a} = (\frac{2}{3})d_{c-a(xy)} + (\frac{1}{3})d_{c-a(z)}$ is constant; (d) $\overline{Dq}$ is equal to $(\frac{4}{3})\ Dq_{xy} + (\frac{1}{3})Dq_z$; (e) spin–orbit coupling is neglected; (f) the distortion parameter $\theta$ of the $MO_6$ octahedron is defined as $\theta = d_{M-O_{(z)}}/d_{M-O_{(xy)}}$.

The corresponding $\theta$, $\overline{Dq}/B$ diagrams for the $d^4$, $d^5$, $d^6$, $d^7$, and $d^8$ ions when $\theta > 1$ (elongation) are given in Fig. 1.

An elongation of the $MO_6$ coordination octahedron can induce such specific $3d$ configurations as high-spin $Fe^{4+}$ $(t_{2g}^3d_{z^2}^1)$ $(^5A_{1g})$, low-spin $Co^{4+}$ $(d_{yz}^2d_{zx}^2d_{xy}^1)(^2B_{2g})$, $Co^{3+}$ with an intermediate electronic configuration $(d_{yz}^2d_{zx}^2d_{xy}^1d_{z^2}^1d_{x^2-y^2}^0)(^3B_{2g})$, low-spin $Ni^{3+}(t_{2g}^6d_{z^2}^1)(^2A_{1g})$, or low-spin $Cu^{3+}(t_{2g}^6d_{z^2}^2$ $d_{x^2-y^2}^0)(^1A_{1g})$.

The energy gain in $\overline{Dq}/B$) units

$$\eta(\theta) = (E/B(\theta) - E/B(1))/(\overline{Dq}/B)$$

resulting from the stabilizing effect of such an elongation appears in Fig. 2.

* Dedicated to Dr. M. J. Sienko.



0022-4596/84 $3.00

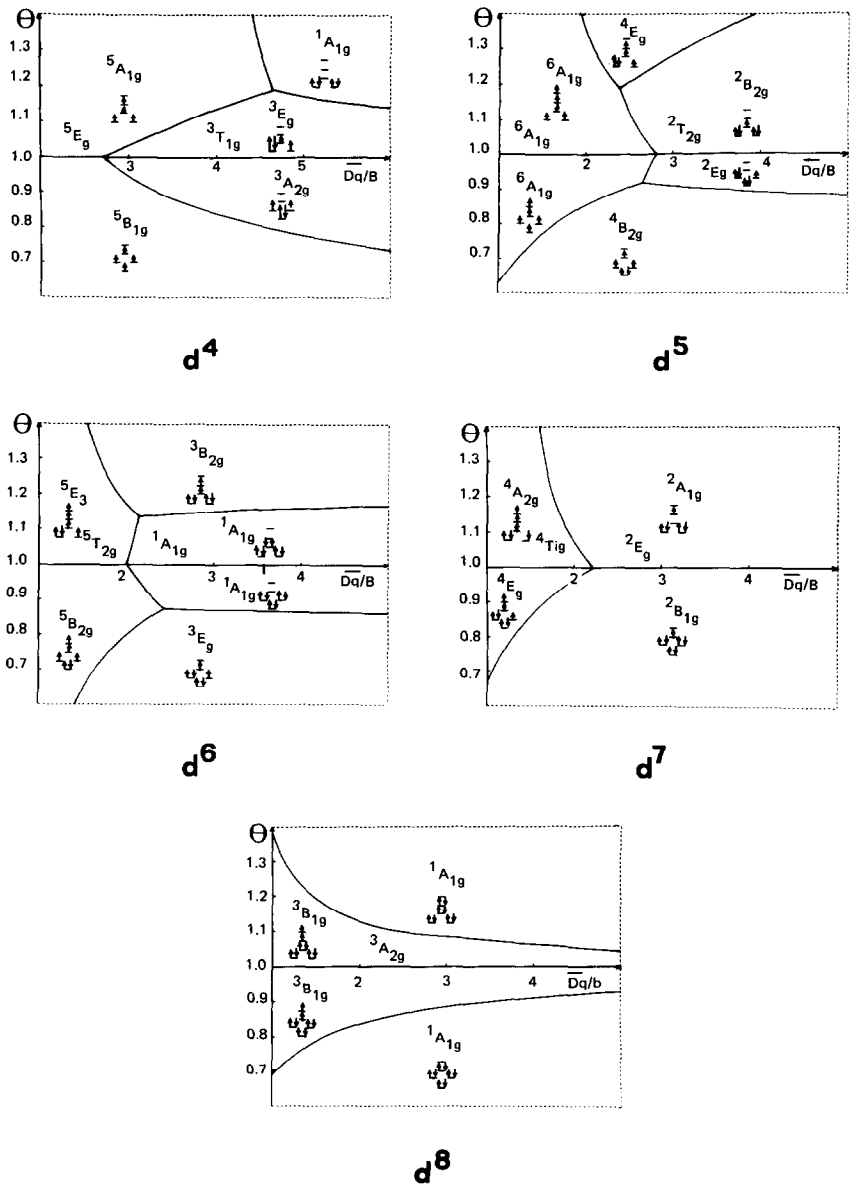


FIG. 1. $\theta$, $\overline{Dq}/B$ diagrams for $d^4$, $d^5$, $d^6$, $d^7$, and $d^8$ cations in a tetragonally distorted octahedral environment.

To check such a model, oxides are required whose structure and composition may favor an elongation of the $MO_6$ octahedron.

In principle, a distortion of the $MO_6$ octahedron along one of its axes ($0z$) is possible in an oxide with a layer structure. We have therefore chosen oxides of $K_2NiF_4$-type structure in which perovskite layers alternate with rocksalt ones (*2*). An elongation of the $MO_6$ octahedra can be produced in the lattice by increasing the covalency of

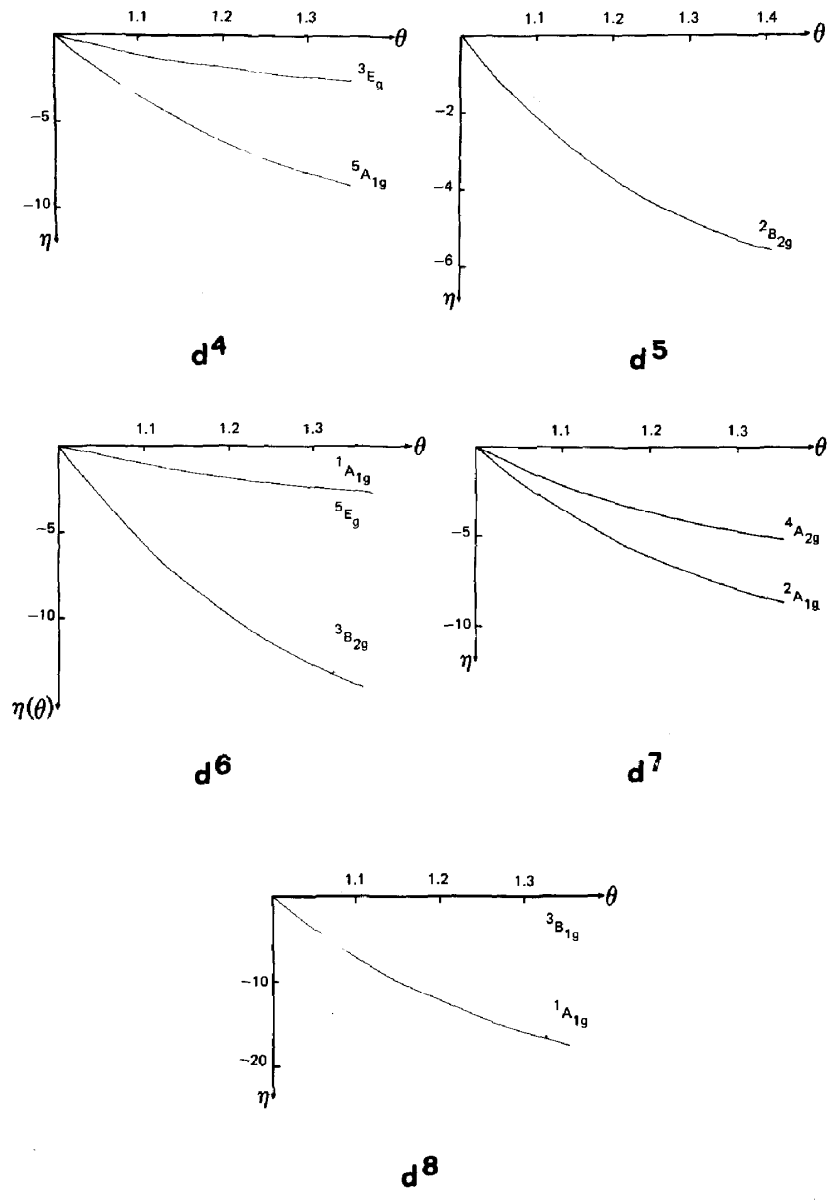


FIG. 2. The energy gain $\eta$ in $\overline{Dq}/B$ units vs elongation $\theta$ for high-spin $d^4(^5A_{1g})$, low-spin $d^5(^2B_{2g})$, medium spin $d^6(^3B_{2g})$, low-spin $d^7(^2A_{1g})$, and low-spin $d^8(^1A_{1g})$.

the $M$–O bonds in the $xy$ perovskite planes. The $M$–O–$M$ angle between adjacent $MO_6$ octahedra is 180° so that the same $2p$ orbital of oxygen is shared between two neighboring $M$-O bonds. Any weakening of a $M$–O bond increases the covalency of the competing $M$–O bond. Thus four weak Li–O bonds in the $xy$ perovskite planes will increase the elongation along the $0z$ axis (Fig. 3). This in turn leads to $A'_xA_{2-x}Li_{0.5}M_{0.5}O_4$ as the suitable stoichiometry.

In this paper we describe the preparation

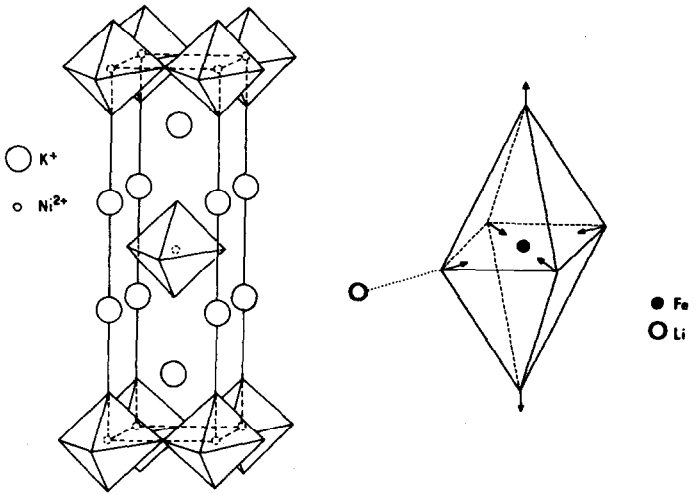


FIG. 3. (a) The $K_2NiF_4$-type structure. (b) The elongation of the $MO_6$ octahedra induced by the square-planar environment constituted by four Li–O bonds.

of $A_{0.5}La_{1.5}Li_{0.5}Fe_{0.5}O_4$ ($A$ = Ca, Sr, Ba), $Sr_{0.5}La_{1.5}Li_{0.5}Co_{0.5}O_4$, $La_2Li_{0.5}Co_{0.5}O_4$, $La_2Li_{0.5}Ni_{0.5}O_4$, and $La_2Li_{0.5}Cu_{0.5}O_4$, and the physical characterization of the electronic configuration of the transition-metal ions ($Fe^{4+}$, $Co^{4+}$, $Co^{3+}$, $Ni^{3+}$, $Cu^{3+}$). The oxidation states of the 3*d* elements have been checked by dissolving the oxides in an acidifed KI solution and redox titration.

X-Ray powder diffraction confirmed the tetragonal $K_2NiF_4$-type structure (Table I). However, the weak additional reflections present in the Guinier photographs of most of the phases point to a larger unit-cell ($a = a_0$ ($K_2NiF_4$) $\sqrt{2}$, $c = c_0$ ($K_2NiF_4$)); consequently they suggest 1–1 $M$/Li ordering in the perovskite planes. The existence of two-dimensional $Li^+/Co^{3+}$ ordering has been supported by a recent electron-diffraction study of $La_2Li_{0.5}Co_{0.5}O_4$ (*3*).

TABLE I

PARAMETERS OF THE TETRAGONAL $K_2NiF_4$-TYPE CELL FOR THE $(A'_xA_{2-x}Li_{0.5}M_{0.5}O_4$ PHASES

| Phases | $a_0$ (Å) | $c_0$ (Å) | $c_0/a_0$ |
|---|---|---|---|
| $Ca_{0.5}La_{1.5}Li_{0.5}Fe_{0.5}O_4$ | 3.73 | 12.84 | 3.44 |
| $Sr_{0.5}La_{1.5}Li_{0.5}Fe_{0.5}O_4$ | 3.76 | 13.03 | 3.46 |
| $Ba_{0.5}La_{1.5}Li_{0.5}Fe_{0.5}O_4$ | 3.78 | 13.14 | 3.47 |
| $Sr_{0.5}La_{1.5}Li_{0.5}Co_{0.5}O_4$ | 3.76(2) | 12.66 | 3.36 |
| $La_2Li_{0.5}Co_{0.5}O_4$ | 3.78(4) | 12.62(4) | 3.3 |
| $La_2Li_{0.5}Ni_{0.5}O_4$ | 3.75(6) | 12.87 | 3.43 |
| $La_2Li_{0.5}Cu_{0.5}O_4$ | 3.73 | 13.20 | 3.54 |

## A. Stabilization of High-Spin $Fe^{4+}$ in $A_{0.5}La_{1.5}Li_{0.5}Fe_{0.5}O_4$ ($A$ = Ca, Sr, Ba)

The axial ratio $c_0/a_0 \simeq 3.46$ suggests a Jahn–Teller configuration $t_{2g}^3 d_{z^2}^1$. The three oxides are antiferromagnetic at low temperature, with $T_N$ between 28 and 35 K (Fig. 4).

The experimental value of the Curie constant ($C \simeq 3 \pm 0.05$) in the paramagnetic region agrees well with the theoretical value ($C = 3$) for four unpaired electrons with a spin-only contribution and confirms the high-spin state for $Fe^{4+}(t_{2g}^3 e_g^1)$ (ground term $^5A_{1g}$) (Table II) (*4*).

Mössbauer resonance spectra of powder samples at room temperature and in the 4.2–35 K range are shown in Fig. 5. The isomer shift at 292 K ($\delta \simeq -0.19$ mm ·

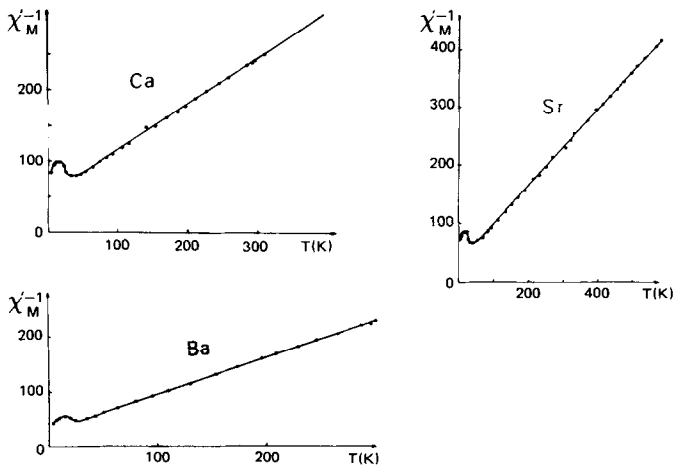


FIG. 4. Reciprocal molar susceptibility vs temperature for $M_{0.5}La_{1.5}Li_{0.5}Fe_{0.5}O_4$ phases ($M$ = Ca, Sr, Ba).

$sec^{-1}$) is smaller than that observed for $Fe^{2+}$ ($\delta \simeq +1.2$ mm · $sec^{-1}$) or $Fe^{3+}$ ($\delta \simeq +0.35$ mm · $sec^{-1}$) with an oxygen 6-coordination. This discrepancy is consistent with a reduced $d$-electron screening effect and thus with the $Fe^{4+}$ oxidation state. The high-spin

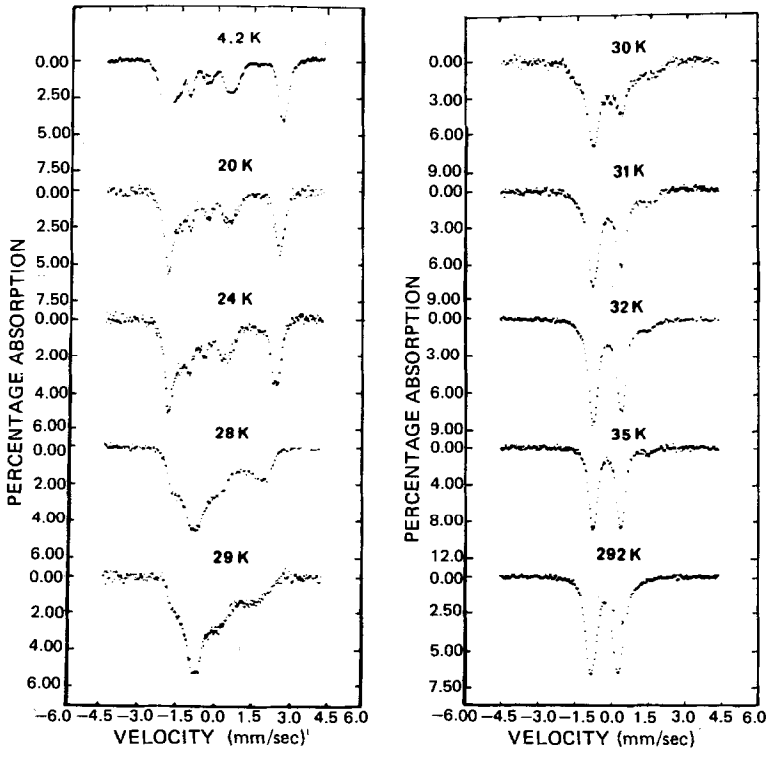


FIG. 5. Mössbauer spectra of $Sr_{0.5}La_{1.5}Li_{0.5}Fe_{0.5}O_4$.

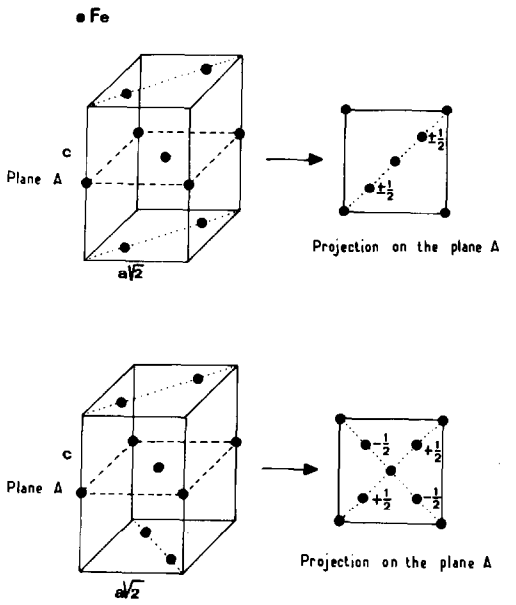


FIG. 6. The two environments of high-spin $Fe^{4+}$ in $M_{0.5}La_{1.5}Li_{0.5}Fe_{0.5}O_4$ phases according to stacking faults along the $c$ axis.

state is confirmed by the difference between the values observed for $A_{0.5}La_{1.5}Li_{0.5}Fe_{0.5}O_4$ ($\delta \simeq -0.19$ mm · $sec^{-1}$) and that for $SrFeO_3$ ($\delta \simeq 0.0$ mm · $sec^{-1}$) where the $Fe^{4+}$ configuration has itinerant $\sigma$-bonding electrons and may be low spin (*5, 6*).

The large quadrupole splitting ($\Delta \simeq 1.10$ mm · $sec^{-1}$) may be explained by the large elongation of the $FeO_6$ octahedron (i.e., $c_0/a_0 = 3.46$). A better fit to the observed spectrum is obtained by assuming two types of

TABLE II

ELECTRONIC CONFIGURATIONS CORRESPONDING TO THE TERMS IN A $D_{4h}$ SYMMETRY

| $O_h$ | $D_{4h}$ | Electronic configuration |
|---|---|---|
| $^5E_g$ | $^5B_{1g}$ | $d^1_{zx}d^1_{yz}d^1_{xy}d^0_{z^2}d^1_{x^2-y^2}$ |
| | $^5A_{1g}$ | $d^1_{zx}d^1_{yz}d^1_{xy}d^1_{z^2}d^0_{x^2-y^2}$ |
| $^3T_{1g}$ | $^3A_{2g}$ | $d^1_{zx}d^1_{yz}d^2_{xy}d^1_{z^2}d^0_{x^2-y^2}$ |
| | $^3E_g$ | $(d_{zx}d_{yz})^3d^1_{xy}d^0_{z^2}d^0_{x^2-y^2}$ |

$Fe^{4+}$ sites with slightly different hyperfine parameters (Table III) (*7*). This assumption could be justified by the presence of stacking faults along the $Oz$ axis and hence the existence of two types of $Fe^{4+}$ environments (Fig. 6). This has been confirmed by a neutron-diffraction study of $Sr_{0.5}La_{1.5}Li_{0.5}Fe_{0.5}O_4$ (*8*) giving $d(Fe\text{–}O)_{Oz}/d(Fe\text{–}O)_{xy} \simeq 1.25$ and $\mu_{Fe} = 3.5\ \mu_B$ (*9*).

### B. Stabilization of Low-Spin $Co^{4+}$ in $Sr_{0.5}La_{1.5}Li_{0.5}Co_{0.5}O_4$

The room-temperature ratio $c/a = 3.36$ is intermediate between that generally observed for an anisotropic electronic configuration, 3.25–3.30 and that characterizing a Jahn–Teller distortion, 3.45. This suggests an anisotropic distribution in the $t_{2g}$ orbitals, $d^2_{yz}d^2_{zx}d^1_{xy}$ and low-spin $Co^{4+}$.

The magnetic behavior follows a Curie–Weiss law between 50 and 200 K (Fig. 7);

TABLE III

MÖSSBAUER PARAMETERS OF THE SPECTRA OF Fe(IV) IN $Sr_{0.5}La_{1.5}Li_{0.5}Fe_{0.5}O_4$

| $T$ (K) | Site 1 | | | Site 2 | | |
|---|---|---|---|---|---|---|
| | $\delta_{\alpha Fe}$ (mm $sec^{-1}$) | $\Delta$ (mm $sec^{-1}$) | $H_{hf}$ (kG) | $\delta_{\alpha Fe}$ (mm $sec^{-1}$) | $\Delta$ (mm $sec^{-1}$) | $H_{hf}$ (kG) |
| 4.2 | −0.10 | 0.99 | 153 | −0.06 | 1.31 | 131 |
| 35 | −0.10 | 0.99 | | −0.11 | 1.28 | |
| 292 | −0.18 | 0.99 | | −0.19 | 1.28 | |

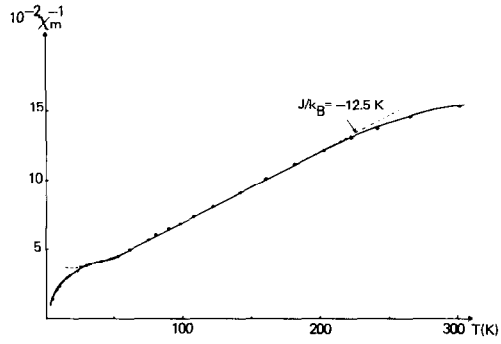


FIG. 7. Reciprocal molar susceptibility vs temperature for $Sr_{0.5}La_{1.5}Li_{0.5}Co_{0.5}O_4$.

the experimental Curie constant ($C = 0.40$) (*5*)) is close to the theoretical value for one unpaired electron ($C = 0.375$). This result is accounted for by the axial field component resulting from the elongation of the $CoO_6$ octahedra along the $0z$ axis. Such a distortion lifts the orbital degeneracy of the $^2T_{2g}$ term to give, in a $D_{4h}$ symmetry, an orbital singlet $^2B_{2g}$ as ground term (Table IV) and tends to decrease the temperature dependence of the magnetic moment toward spin-only value.

An interpretation of the magnetic behavior of $Sr_{0.5}La_{1.5}Li_{0.5}Co_{0.5}O_4$, which takes into account a modified Kotani's Hamiltonian resulting from the anisotropic field and the bidimensional character of this structure, leads to a calculated value of the exchange integral ($J/k_B$) close to $-12.5$ K. Owing to the expected high covalency of the $Co^{4+}$–O bond, this small value can be explained by the observed $Li^+/Co^{4+}$ 1–1 ordering, which leads to weak magnetic superexchange interactions between $Co^{4+}$ ions (*10*).

TABLE IV

ELECTRONIC CONFIGURATIONS CORRESPONDING TO THE TERMS IN $D_{4h}$ SYMMETRY FOR A $d^5$ CATION

| $O_h$ | $D_{4h}$ | Electronic configurations |
|---|---|---|
| $^6A_{1g}$ | $^6A_{1g}$ | $d^1_{zx}d^1_{yz}d^1_{xy}d^1_{z^2}d^1_{x^2-y^2}$ |
| $^4T_{1g}$ | $^4A_{2g}$ | $d^1_{zx}d^1_{yz}d^2_{xy}d^1_{z^2}d^0_{x^2-y^2}$ |
| | $^4E_g$ | $(d_{zx}d_{yz})^3d^1_{xy}d^1_{z^2}d^0_{x^2-y^2}$ |
| $^2T_{2g}$ | $^2E_g$ | $(d_{zx}d_{yz})^3d^2_{xy}d^0_{z^2}d^0_{x^2-y^2}$ |
| | $^2B_{2g}$ | $d^2_{zx}d^2_{yz}d^1_{xy}d^0_{z^2}d^0_{x^2-y^2}$ |

TABLE V

ELECTRONIC CONFIGURATIONS CORRESPONDING TO THE TERMS IN $D_{4h}$ SYMMETRY FOR A $d^6$ CATION

| $O_h$ | $D_{4h}$ | Electronic configurations |
|---|---|---|
| $^1A_{1g}$ | $^1A_{1g}$ | $(d^2_{xz}d^2_{xy}d^2_{yz}d^0_{z^2}d^0_{x^2-y^2})$ or $(e^4_gb^2_{2g}a^0_{1g}b^0_{1g})$ |
| $^5T_{2g}$ | $^5B_{2g}$ | $(d^1_{xz}d^1_{yz}d^2_{xy}d^1_{z^2}d^1_{x^2-y^2})$ or $(e^2_gb^2_{2g}a^1_{1g}b^1_{1g})$ |
| | $^5E_g$ | $(d^2_{xz}d^1_{yz}d^1_{xy}d^1_{z^2}d^1_{x^2-y^2})$ or $(e^3_gb^1_{2g}a^1_{1g}b^1_{1g})$ |
| $^3T_{2g}$ | $^3E_g$ | $(d^2_{xz}d^1_{yz}d^2_{xy}d^0_{z^2}d^1_{x^2-y^2})$ or $(e^3_gb^2_{2g}a^0_{1g}b^1_{1g})$ |
| | $^3B_{2g}$ | $(d^2_{xz}d^2_{yz}d^1_{xy}d^1_{z^2}d^0_{x^2-y^2})$ or $(e^4_gb^1_{2g}a^1_{1g}b^0_{1g})$ |

An ESR investigation at 4.2 K confirms the anisotropic electronic configuration of $Co^{4+}$ ($2.32 < g_\perp < 2.55$, $g_\parallel < 0.85$). The calculated value of the $k$ factor ($k = 0.65$) which is much smaller than that observed in $Al_2O_3:Co^{4+}$ ($0.94 < k < 1.00$), can be explained by the enhancement of the covalency of the $Co^{4+}$–O bond arising from the square-planar surrounding formed by the four weak competing Li–O bonds.

### C. Stabilization of a Medium Electronic Configuration of $Co^{3+}$

In an oxygen lattice of $O_h$ symmetry the crystal-field splitting of $Co^{3+}$ is close to the exchange energy. Such a competition favors the low-spin state ($t^6_{2g}e^0_g$) at low temperature and a low-spin ($^1A_{1g}$, $S = 0$) $\rightarrow$ high-spin ($^5T_{2g}$, $S = 2$) transition at higher temperature (*11–15*).

For $O_h$ symmetry the energy of the cubic field term vs $Dq/B$ is given by the Tanabe–Sugano diagram (*16*). For a $D_{4h}$ elongation splitting of the high-energy $^3T_{2g}$ term ($S = 1$), (Table V) can lead to the stabilized $^3B_{2g}$ term having an energy close to that of the $^1A_{1g}$ term, or even becoming the ground term (Fig. 8).

In $SrLaCoO_4$ with $K_2NiF_4$-type structure, the structural distortion is too small

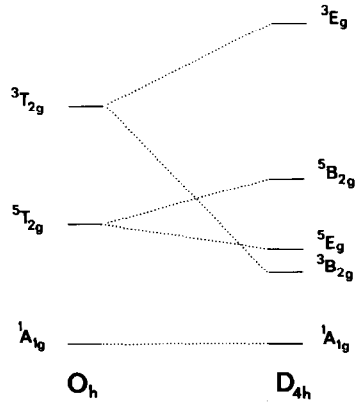


FIG. 8. Evolution of the relative stability of the terms vs distortion.

($c_0/a_0 = 3.29$, $\theta = 1.07$) to stabilize such an intermediate configuration (*15*). However, the $La_2Li_{0.5}Co_{0.5}O_4$ phase, where the weak Li–O bonds increase the covalency of the Co–O bonds in the perovskite planes, might be able to induce a sufficient elongation of the $CoO_6$ octahedra. The observed $c_0/a_0$ ratio at room temperature, which is close to 3.33, does not permit to conclude in favor of an anisotropic, medium-spin configuration ($d^2_{yz}d^2_{zx}d^1_{xy}d^1_{z^2}d^0_{x^2-y^2}$) for some $Co^{3+}$ ions, although the increase of the $c_0/a_0$ ratio-vs-temperature curve suggests such an intermediate-spin state may contribute to the spin transition. The magnetic curve $\chi_M^{-1} = f(T)$ indicates the onset of a spin transition at 200 K (*17*). At low temperature $Co^{3+}$ is in a diamagnetic low-spin state; a small amount of paramagnetic $Co^{3+}$ or of impurities causes the experimental curve to shift toward lower $\chi_M^{-1}$ values below room temperature (Fig. 9).

The observed $\chi_M$ value can be represented by

$$\chi_M = A + B + C + Y(T)/2T$$

where $A$ stands for the diamagnetic contribution $\chi_{dia.}$ of all present ions, $B$ is the Van Vleck paramagnetism $N\alpha$, which for $^1A_{1g}$ assumes the value $8N\beta^2/10Dq$. $C$ is a small contribution due to magnetic $Co^{3+}$ or magnetic impurities. $Y$ corresponds to the Boltzmann distribution between the ground term $^1A_{1g}$ and the term involved in the spin transition. A low-spin ($^1A_{1g}$) to a medium-spin ($^3B_{2g}$) transition, with a splitting $\Delta_1$, does not yield a good fit to the experimental magnetic curve. However, a good agreement is obtained when a second low-spin → high-spin transition ($^1A_{1g} \rightarrow {}^5E_g$), with a splitting $\Delta_2$ is added using $\Delta_1 = 1600$ cm$^{-1}$ and $\Delta_2 = 1650$ cm$^{-1}$.

To improve the $D_{4h}$ elongation of the $CoO_6$ octahedra, a small amount ($x = 0.1$) of $Cu^{3+}$ (low-spin $d^8$) in $La_2Li_{0.5}Cu_{0.5}O_4$ ($c/a = 3.54$) was replaced by $Co^{3+}$ (*18*). Using the above model to fit the magnetic curve resulted in a much smaller $^1A_{1g} \rightarrow {}^3B_{2g}$ splitting with $\Delta_1 = 500$ cm$^{-1}$ (Fig. 10). It appears that it should be possible to stabilize the medium-spin state of $Co^{3+}$, with $^3B_{2g}$ as ground term from the room temperature in a square-planar environment.

### D. Stabilization of Low-Spin $Ni^{3+}$ in $La_2Li_{0.5}Ni_{0.5}O_4$

Due to its high crystal-field stabilization energy, $Ni^{3+}$ in an oxygen lattice is in a low-

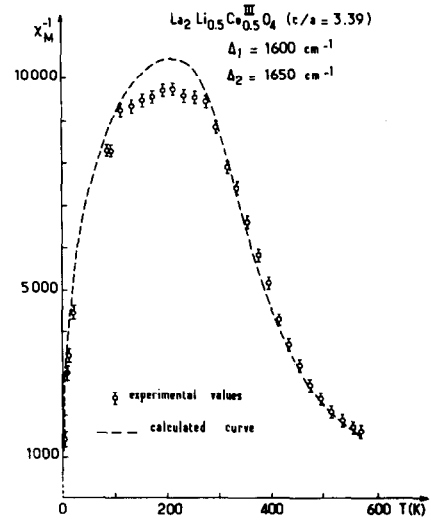


FIG. 9. Comparison of experimental and theoretical values of $\chi_M = f(T)$ for $La_2Li_{0.5}Co_{0.5}O_4$.

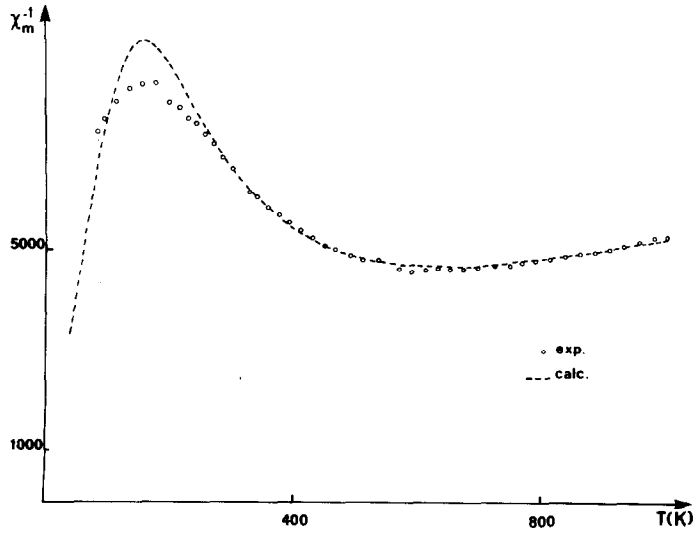


FIG. 10. Comparison of experimental and theoretical values of $\chi_M = f(T)$ for $La_2Li_{0.5}Cu_{0.4}Co_{0.1}O_4$.

spin state, $t_{2g}^6 d_{z^2}^1$. This is, for example, the situation in the $LnNiO_3$ perovskites (*19*) or in the $SrLnNiO_4$ phases with $K_2NiF_4$-type structure (*20*), but the high covalency of the $Ni^{3+}$–O bond leads to some electronic delocalization and may induce some metallic behavior. However, the two-dimensional 1–1 $Li^+$–$Ni^{3+}$ ordering in the perovskite layers of $La_2Li_{0.5}Ni_{0.5}O_4$ makes possible the characterization of the "localized" low-spin state (*21*).

The observed *c*/*a* ratio, which is close to

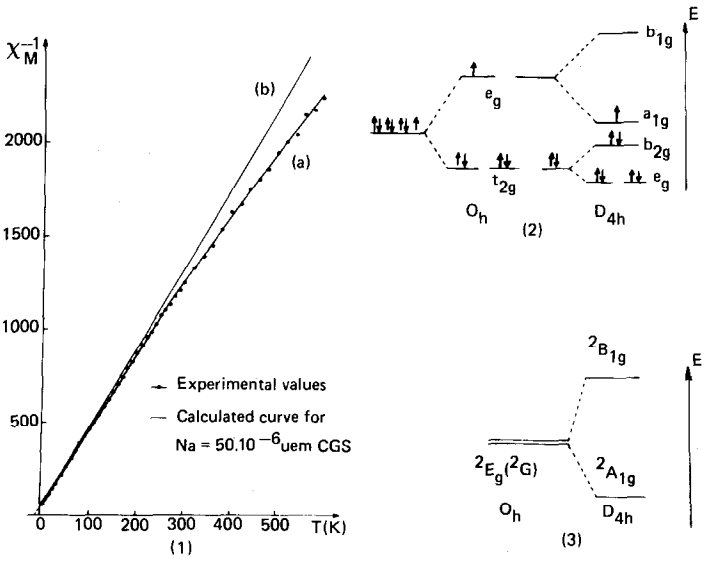


FIG. 11. (1) Reciprocal molar susceptibility vs temperature for $La_2Li_{0.5}Ni_{0.5}O_4$. (2) Energy diagram of $Ni^{3+}$ *d* orbitals. (3) Splitting of the ground term of $Ni^{3+}$ in a $D_{4h}$ symmetry.

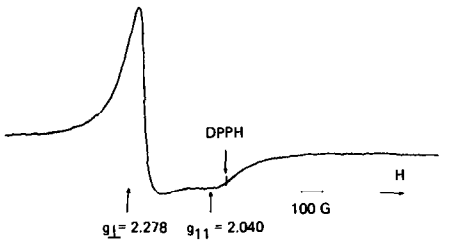


FIG. 12. ESR spectrum of $La_2Li_{0.5}Ni_{0.5}O_4$ at room temperature.

3.43, is consistent with the presence of a Jahn–Teller distortion arising from the $t_{2g}^6 d_{z^2}^1$ configuration. The difference between the Curie constant $C \simeq 0.466 \pm 0.010$ determined from the magnetic curve, and the theoretical value of 0.375 for $Ni^{3+}$ is attributable to the $D_{4h}$ symmetry of the $Ni^{3+}$ site which induces anisotropy in the molar magnetic susceptibility (Fig. 11).

The ESR spectrum at 300 K (Fig. 12) is consistent with an anisotropic electronic configuration: $g_\parallel = 2.040$, $g_\perp = 2.278$. It agrees well with the structural elongation and with the anisotropy of the susceptibility ($g_\perp > g_\parallel$). A recent ESR study (*3*) of low-spin $Ni^{3+}$ in an oxide of $K_2NiF_4$ type, $SrLaAl_{1-x}Ni_xO_4$, gave $g_\perp = 2.18$ and $g_\parallel = 2.01$ for $x = 0.25$. The increased elongation along the *0z* axis of the $NiO_6$ octahedra, induced by the weak competing Li–O bonds, may be responsible for the larger difference between $g_\perp$ and $g_\parallel$ in $La_2Li_{0.5}Ni_{0.05}O_4$.

### E. The $d^8$ Low-Spin State of $Cu^{3+}$ in $La_2Li_{0.5}Cu_{0.5}O_4$

Oxides containing $Cu^{3+}$ occur very seldom. The phases $MCuO_2$ ($M$ = Na, K, Rb, Cs) and $Na_3CuO_3$ have been described earlier (*22–25*). More recently the rhombohedral perovskite $LaCuO_3$ has been synthesized under a high oxygen pressure (*26*). It is likely that $Cu^{3+}$ in this compound is stabilized by electron delocalization, characterized by narrow-band Pauli paramagnetism (*27*).

$Cu^{3+}$ in a low-spin state $d^8$ has now been stabilized in the $La_2Li_{0.5}Cu_{0.5}O_4$ phase as the result of the induced elongation of the $CuO_6$ octahedron. The $c/a$ ratio (3.54) is the highest so far observed for a $K_2NiF_4$ structure; it suggests a Jahn–Teller distortion higher than that due to only one unpaired electron in the $e_g$ orbitals; it is consistent with a low-spin $d^8$ state, $t_{2g}^6 d_{z^2}^2 d_{x^2-y^2}^0$. The diamagnetic behavior confirms this electronic configuration (*26*).

## Conclusion

As shown by the various examples above (high-spin $Fe^{4+}$-$d^4$, low-spin $Co^{4+}$-$d^5$, medium-spin $Co^{3+}$-$d^6$, low-spin $Ni^{3+}$-$d^7$, low-spin $Cu^{3+}$-$d^8$), the $A_2Li_{0.5}M_{0.5}O_4$ matrix appears to be particularly suitable for the stabilization of anisotropic electron configurations. The present study is a good illustration of the correlations between structural and chemical-bonding factors of the near-neighbor oxygen environment of a transition element ion determine the electronic configuration adopted.

## Acknowledgments

The authors are grateful to Dr. N. Chevreau, Dr. J. F. Colombet, Dr. J. M. Dance, Dr. L. Fournes, Dr. J. L. Marty, Dr. F. Menil, Dr. C. Parent, and Dr. J. L. Soubeyroux for their contributions to these studies.

## References

1. B. BUFFAT, G. DEMAZEAU, M. POUCHARD, AND P. HAGENMULLER, *Proc. Indian Acad. Sci. (Chem. Sci.)* **93,** 313 (1984).
2. G. LE FLEM, G. DEMAZEAU, AND P. HAGENMULLER, *J. Solid State Chem.* **44,** 82 (1982).
3. R. A. MOHAN RAM, K. K. SINGH, W. H. MADHUSUDAN, P. GANGULY, AND C. N. R. RAO, *Mater. Res. Bull.* **18,** 703 (1983).
4. G. DEMAZEAU, M. POUCHARD, N. CHEVREAU, M. THOMAS, F. MENIL, AND P. HAGENMULLER, *Mater. Res. Bull.* **16,** 689 (1981).

5. P. K. GALLAGHER, J. B. MAC CHESNEY, AND D. N. E. BUCHANAN, *J. Chem. Phys.* **41**(8), 2429 (1964).
6. H. ODA, Y. YAMAGUCHI, M. TAKEI, AND H. WATANABE, *J. Phys. Colloq. Cl. Suppl. No. 4* **38**, C1-121 (1977).
7. M. F. THOMAS, G. DEMAZEAU, M. POUCHARD, AND P. HAGENMULLER, *Solid State Commun.* **39**, 751 (1981).
8. J. L. SOUBEYROUX, N. CHEVREAU, G. DEMAZEAU, M. POUCHARD, AND P. HAGENMULLER, *J. Solid State Chem.* **51**, 38 (1984).
9. J. L. SOUBEYROUX, B. BUFFAT, N. CHEVREAU, AND G. DEMAZEAU, *Physica B* **120**, 227 (1983).
10. B. BUFFAT, G. DEMAZEAU, M. POUCHARD, J. M. DANCE, AND P. HAGENMULLER, *J. Solid State Chem.* **50**, 33 (1983).
11. G. BLASSE, *J. Appl. Phys.* **36**, 879 (1965).
12. P. M. RACCAH AND J. B. GOODENOUGH, *Phys. Rev.* **155**, 932 (1967).
13. V. G. BHIDE, D. S. RAJORIA, G. RAMA RAO, AND C. N. R. RAO, *Phys. Rev. B* **6**, 1021 (1972).
14. G. DEMAZEAU, M. POUCHARD, AND P. HAGENMULLER, *J. Solid State Chem.* **9**, 202 (1974).
15. G. DEMAZEAU, PH. COURBIN, G. LE FLEM, M. POUCHARD, AND P. HAGENMULLER, *Nouv. J. Chim.* **3**, 171 (1979).
16. Y. TANABE AND S. SUGANO, *J. Phys. Soc. Jpn.* **753**, 766 (1954).
17. G. DEMAZEAU, M. POUCHARD, M. THOMAS, J. F. COLOMBET, J. C. GRENIER, L. FOURNES, J. L. SOUBEYROUX, AND P. HAGENMULLER, *Mater. Res. Bull.* **15**, 451 (1980); **16**, 353 (1981).
18. B. BUFFAT, G. DEMAZEAU, M. POUCHARD, AND P. HAGENMULLER, *Mater. Res. Bull.* **18**, 1153 (1983).
19. G. DEMAZEAU, A. MARBEUF, M. POUCHARD, AND P. HAGENMULLER, *J. Solid State Chem.* **3**, 582 (1971).
20. G. DEMAZEAU, M. POUCHARD, AND P. HAGENMULLER, *J. Solid State Chem.* **18**, 159 (1976).
21. G. DEMAZEAU, J. L. MARTY, M. POUCHARD, T. ROJO, J. M. DANCE, AND P. HAGENMULLER, *Mater. Res. Bull.* **16**, 47 (1981).
22. W. KLEMM, G. WEHRMEYER, AND H. BADE, *Z. Elecktrochem. Ber. Bunsenges. Phys. Chem.* **63**, 56 (1959).
23. K. HESTERMANN AND R. HOPPE, *Z. Anorg. Allg. Chem.* **367**, 261 (1969).
24. K. HESTERMANN AND R. HOPPE, *Z. Anorg. Allg. Chem.* **367**, 249 (1969).
25. K. HESTERMANN AND R. HOPPE, *Z. Anorg. Allg. Chem.* **367**, 270 (1969).
26. G. DEMAZEAU, C. PARENT, M. POUCHARD, AND P. HAGENMULLER, *Mater. Res. Bull.* **7**, 913 (1972).
27. J. B. GOODENOUGH, N. F. MOTT, M. POUCHARD, G. DEMAZEAU, AND P. HAGENMULLER, *Mater. Res. Bull.* **8**, 647 (1973).